Treatment of nanofluid within porous media using non-equilibrium approach

Ahmad Shafee[1] · Behnoush Rezaeianjouybari[2] · Iskander Tlili[3,4]

Abstract

Lorentz force impact on heat transfer was scrutinized in current paper, and nanomaterial behavior was analyzed within a domain which has been scrutinized via non-equilibrium theory. Moreover, radiation term has been added and shape factor impact was investigated. Outputs reveal that suppression of convective flow in appearance of Lorentz forces makes Nu_{ave} to decline. More complex isotherms generate with rise of Ra; thus, Nu_{ave} augments with enhancement of Ra. Nu_{ave} is a reduction function of Nhs, while Rd has opposite relation.

Keywords Non-equilibrium · Nanofluid · Lorentz force · Porous · CFD

Introduction

In energy-saving systems and industry, increasing the heat transfer rate in convective streams is imperative. Heat transfer is very practical in different applications such as renewable energy units, cooling systems, electronic cooling devices, etc., and those systems typically apply forced or natural convection by using typical fluids such as oil, air or water. Recently, nanofluid technology has been presented as a promising method for increasing thermophysical features of testing fluids by suspending nanopowders in the typical fluids [1–16]. Guestala et al. [17] scrutinized the free convection of NFs within a cylindrical tank. They found that the heat transfer grew when Re, particles volume fraction or the heated length increases. Simulation of nanomaterial treatment becomes popular in recent decade [18–35]. Selimifendigil et al. [36] numerically analyzed the mixed convection including an internal rotating

cylindrical a permeable layer accumulated with covered NFs. Based on their results, heat transfer grew when the cylinder's angular velocity rose. The evacuated tube including mini-CPC reflectors has been studied by Korrees et al. [37] who used Solidworks flow simulation software for simulating. They estimated the temperature of receiver and the thermal output of each module. Numerical approaches are extended by reviewers to find the performance of systems [38–56]. Several researchers studied the effect of nanofluid on renewable energy systems. The impact of Al_2O_3–H_2O nanofluids on the performance of flat sheet photovoltaic thermal collectors was investigated by Bianco et al. [57]. Both microscopic [58, 59] and macroscopic [60–75] approaches can predict behavior of nanofluid. Hossain and Rees [76] scrutinized the free convective stream of a viscous liquid in an oblong cavity heated from bottom. They applied upwind differential process. In addition, they surveyed zero Darcy inversion terms in this study. Based on their results, cell shape in the tank is a feature of Grashof number and tank aspect ratio. Impact of thermophoresis and nanoflid features on thermal efficiency has been analyzed by Astanina et al. [77] who found that the intensification of stream in the cavity had inverse relationship with the heater place while it had direct relationship with Re; based on their results, the finest place of the heater was the left surface of considered tank. Also, Aham et al. [78] surveyed optimal features such as transmittance, extinction coefficient and scattering based on metal oxide, metal, graphite and grapheme for using nanofluids in solar thermal systems. Heat transfers along free convection in different fluid stream in a tank as illustrated by

✉ Iskander Tlili
  iskander.tlili@tdtu.edu.vn

[1] Institute of Research and Development, Duy Tan University, Da Nang 550000, Vietnam

[2] Department of Mechanical and Aerospace Engineering, University of Missouri, Columbia, MO 65211, USA

[3] Department for Management of Science and Technology Development, Ton Duc Thang University, Ho Chi Minh City, Vietnam

[4] Faculty of Applied Sciences, Ton Duc Thang University, Ho Chi Minh City, Vietnam

Drummond and Korpela [79] who found that Gr does not rely on boundary conditions because wall stability relies on the shear forces rather than gravity. Additionally, they reported that heat transfer within an adiabatic cavity was higher compared to that of in tank within convective walls.

This article discusses how magnetic force can affect the nanomaterial behavior through a permeable region, and to reduce computational cost, single-phase model has been utilized. Moreover, influence of radiation term was added in equations and several outputs were summarized in result section.

Formula explanation and simulation

In current article, 2D free convection in laminar condition was investigated. As depicted in Fig. 1, wavy wall received uniform heat flux. Geometry has 2 adiabatic walls and outer surface is cold. To evaluate temperature distribution inside the porous solid zones, new scalar was introduced. Overlooking joule heating impact and considering homogeneous carrier fluid leads to below equations [80]:

$$\frac{\partial P}{\partial x} + \frac{\mu_{nf}}{K}u = (\sin\gamma)\sigma_{nf}B_0^2[-u(\sin\gamma) + v(\cos\gamma)] \tag{1}$$

$$\frac{\partial u}{\partial x} + \frac{\partial v}{\partial y} = 0 \tag{2}$$

$$\frac{\partial P}{\partial y} + \frac{\mu_{nf}}{K}v = (T - T_c)g\rho_{nf}\beta_{nf}$$
$$+ (\cos\gamma)\sigma_{nf}B_0^2[u(\sin\gamma) - v(\cos\gamma)] \tag{3}$$

$$\frac{1}{\varepsilon}\left(u\frac{\partial T_{nf}}{\partial x} + v\frac{\partial T_{nf}}{\partial y}\right) + \frac{1}{(\rho C_p)_{nf}}\frac{\partial q_r}{\partial y}$$
$$= \frac{k_{nf}}{(\rho C_p)_{nf}}\left(\frac{\partial^2 T_{nf}}{\partial x^2} + \frac{\partial^2 T_{nf}}{\partial y^2}\right) + \frac{h_{nfs}}{(\varepsilon)(\rho C_p)_{nf}}(-T_{nf} + T_s),$$
$$\left[q_r = -\frac{4\sigma_e}{3\beta_R}\frac{\partial T_{nf}^4}{\partial y}, \; T_{nf}^4 \cong 4T_c^3 T_{nf} - 3T_c^4\right] \tag{4}$$

$$\frac{k_s}{(\rho C_p)_s}\left(\frac{\partial^2 T_s}{\partial x^2} + \frac{\partial^2 T_s}{\partial y^2}\right) + \frac{h_{nfs}}{(1-\varepsilon)(\rho C_p)_s}(T_{nf} - T_s) = 0 \tag{5}$$

In order to simplify the above equations, Eq. (6) has been used:

$$v = -\frac{\partial\psi}{\partial x}, \quad \theta_s = (T_s - T_c)/\Delta T,$$
$$u = \frac{\partial\psi}{\partial y}, \quad \theta_{nf} = (T_{nf} - T_c)/\Delta T,$$
$$Y = yL^{-1}, \; \Delta T = L(k_f)^{-1}q'', \quad X = xL^{-1}$$
$$\Psi = \psi/\alpha_{nf}, \tag{6}$$

By including stream function definition, equations convert to below forms:

$$\frac{\partial^2\Psi}{\partial X^2} + \frac{\partial^2\Psi}{\partial Y^2} = -\frac{A_6}{A_5}\text{Ha}\left[\frac{\partial^2\Psi}{\partial Y^2}(\sin^2\gamma) + \frac{\partial^2\Psi}{\partial X^2}(\cos^2\gamma)\right.$$
$$\left. + 2\frac{\partial^2\Psi}{\partial X\partial Y}(\sin\gamma)(\cos\gamma)\right] - \frac{A_3 A_2}{A_4 A_5}\frac{\partial\theta_{nf}}{\partial X}\text{Ra} \tag{7}$$

$$\varepsilon\left(\left(1 + \frac{4}{3}\left(\frac{k_{nf}}{k_f}\right)^{-1}\text{Rd}\right)\frac{\partial^2\theta_{nf}}{\partial Y^2} + \frac{\partial^2\theta_{nf}}{\partial X^2}\right)$$
$$+ \frac{\partial\Psi}{\partial X}\frac{\partial\theta_{nf}}{\partial Y} + \text{Nhs}(\theta_s - \theta_{nf}) = \frac{\partial\theta_{nf}}{\partial X}\frac{\partial\Psi}{\partial Y} \tag{8}$$

$$\left(\frac{\partial^2\theta_s}{\partial Y^2} + \frac{\partial^2\theta_s}{\partial X^2}\right) + \text{Nhs}\,\delta_s(\theta_{nf} - \theta_s) = 0 \tag{9}$$

In final equations, there exist some new parameters which should be defined as:

$$\text{Ra} = \frac{g\,K(\rho\beta)_f L\,\Delta T}{\mu_f\alpha_f}, \quad A_3 = \frac{(\rho\beta)_{nf}}{(\rho\beta)_f}, \quad A_5 = \frac{\mu_{nf}}{\mu_f},$$
$$A_2 = \frac{(\rho C_P)_{nf}}{(\rho C_P)_f}, \quad A_6 = \frac{\sigma_{nf}}{\sigma_f}, \quad A_4 = \frac{k_{nf}}{k_f},$$
$$A_1 = \frac{\rho_{nf}}{\rho_f}, \quad \text{Ha} = \frac{\sigma_f K B_0^2}{\mu_f}, \quad \text{Rd} = 4\sigma_e T_c^3/(\beta_R k_f)$$
$$\delta_s = [(1-\varepsilon)k_s]^{-1}k_{nf}, \quad \text{Nhs} = (k_{nf})^{-1}h_{nfs}L^2 \tag{10}$$

The boundary conditions are summarized in Fig. 1, and we ignored to write them again, and for estimating rate of heat transfer the below factor has been defined

$$\text{Nu}_{ave} = \frac{1}{S}\int_0^s \text{Nu}_{loc}\,ds, \; \text{Nu}_{loc} = \frac{1}{\theta}\left(1 + \frac{4}{3}\left(\frac{k_{nf}}{k_f}\right)^{-1}\text{Rd}\right)\left(\frac{k_{nf}}{k_f}\right) \tag{11}$$

CuO nanopowders were dispersed into H_2O, and for evaluating the properties same formulation of [80] was employed. In addition, to predict thermal conductivity, shape effect was employed [81]. To simplify the governing equations, vorticity formulations were used and CVFEM was utilized for simulation purpose. This approach was
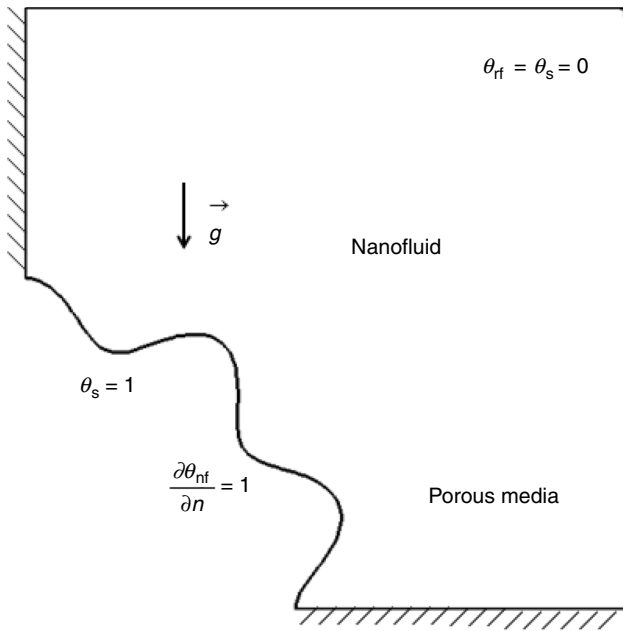
Fig. 1 Geometry of permeable domain with uniform heat flux

introduced first by Sheikholeslami [82] for thermal problems, and he wrote more details in his reference book. In current approach, CVFEM was employed which was utilized for various problems [83–89].

Results and discussion

Non-equilibrium modeling for permeable zone was involved in governing equations and simplified with using vorticity formulation and finally solved via CVFEM in this article. Validation step makes us ensure about the accuracy of used model, and Fig. 2 proves the nice agreement of our written code [90]. To reach the minimum computational costs, grid independency analysis has been analyzed and Table 1 illustrates different values of Nu for different meshes. Impact of dispersing nanopowders and imposing radiation terms are illustrated in Figs. 3 and 4. Inclusion of nanoparticles makes the flow velocity to augment and increases the temperature gradient. The position of therma plume changes with adding nanoparticles, and it shifts to right. The structure of flow is slightly affected by Rd, while according to definition of Nu_{ave}, it has direct relation with Rd.

To evaluate impact of Nhs, Ha and Ra on thermal treatment of working fluid, Figs. 5, 6, 7 and 8 were presented. Steeping of isotherms over wavy wall decreases as magnetic field is imposed and impact of Ha becomes weaker in greater Nhs. With impose of Ha, isotherms become uniform

Table 1 Different mesh and calculated Nu_{ave} when $Ra = 10,000$, $Ha = 20$, $\varepsilon = 0.3$, $Nhs = 10$, $Rd = 0.8$ and $\phi = 0.04$

61×181	81×241
2.99183	3.00129
71×211	91×271
3.01364	3.01554
101×301	
3.01705	
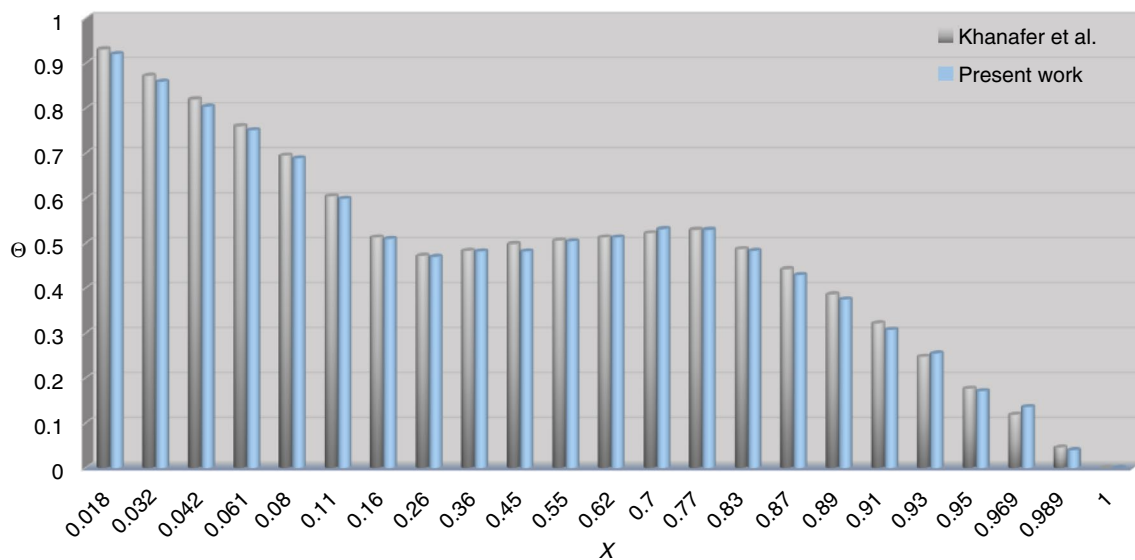
Fig. 2 Demonstrating deviation of present result with [90] when $Gr = 10^4$, $\phi = 0.1$
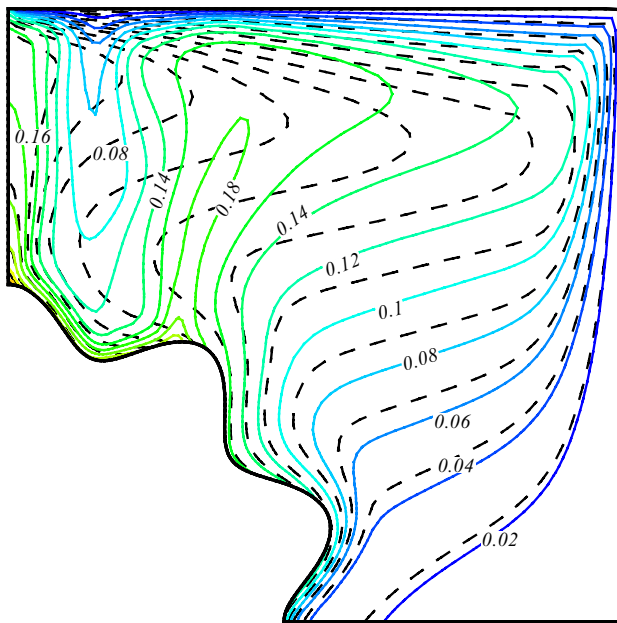
$((\phi = 0.04)\ (\text{—})\ \text{and}\ (\phi = 0)(\text{- - -}))$

Fig. 3 Influences of ϕ on θ_{nf} at Ra $= 10^4$, Nhs $= 10$, $m = 5.7$, Ha $= 0$, $\varepsilon = 0.3$, Rd $= 0.8$

and convection weakens. This is the reason of disappearing thermal plume from with increasing Ha. In the absence of magnetic force and greatest Ra, three cells were established

in domain and two smaller ones create thermal plume due to reverse direction circulation. When Ha is not zero, all cells merged and one weaker cell appears. Nhs has slight impact on nanomaterial behavior in comparison with Hartmann number. As Ha increases, the center of eddy shifted downwards. As Nhs augments, the power of eddies augments and stronger thermal plume appear when Ra $= 10^4$.

Impacts of changing scrutinized parameters on Nu_{ave} are illustrated in Fig. 9. As Nhs augments, temperature gradient deteriorates which indicates lower Nu_{ave}. Magnetic force reduces the nanoparticle velocity and generates thicker boundary layer which results in lower Nu_{ave}. Direct relation exists between Ra and Nu_{ave} which is attributed to thinner boundary layer with augment of Ra. With impose of radiation impact, Nusselt number enhances, but it is no sensible in greatest Nhs. The below equation can present influences of parameters as good mathematic formula.

$$\text{Nu}_{\text{ave}} = 3.02 + 1.62\ \text{Ra}^* - 0.95\ \text{Nhs}^* + 1.35\ \text{Rd} - 1.42\ \text{Ha}^*$$
$$- 1.07\ \text{Ra}^*\text{Nhs}^* - 1.19\ \text{Ra}^*\text{Ha}^*$$
$$- 0.6\ \text{Nhs}^*\text{Rd} + 1.42\ \text{Nhs}^*\ \text{Ha}^* - 0.77\ \text{Ha}^*\ \text{Rd}$$
$$\text{Ra}^* = 10^{-3}\ \text{Ra}, \quad \text{Ha}^* = 0.1\ \text{Ha}, \quad \text{Nhs}^* = 10^{-3}\ \text{Nhs}$$
$$(12)$$

As demonstrated in Table 2, shape of powder can influence the thermal behavior due to its impact on thermal conductivity. As shape factor augments, Nu_{ave} enhances and
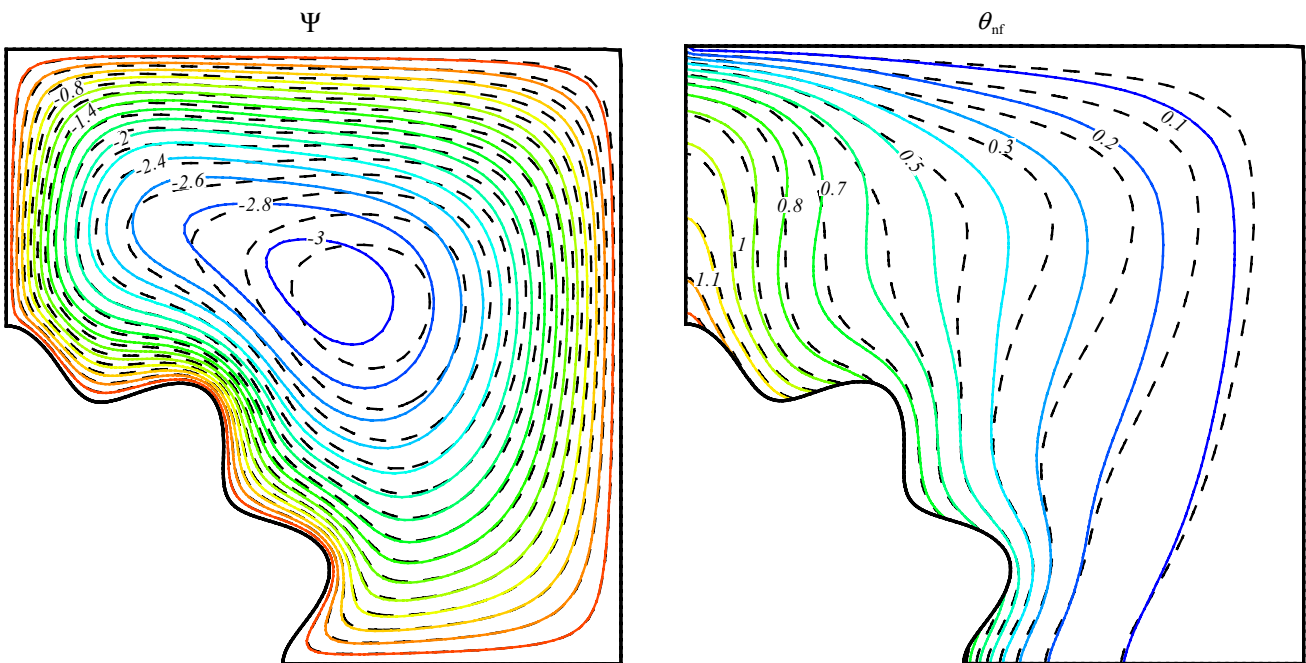
$((\text{Rd} = 0.8)\ (\text{- - -})\ \text{and}\ (\text{Rd} = 0\ )(\text{—}))$

Fig. 4 Influences of Rd on θ_{nf} and Ψ at $\phi = 0.04$, Nhs $= 10$, $\varepsilon = 0.3$, $m = 5.7$, Ra $= 10^4$, Ha $= 20$
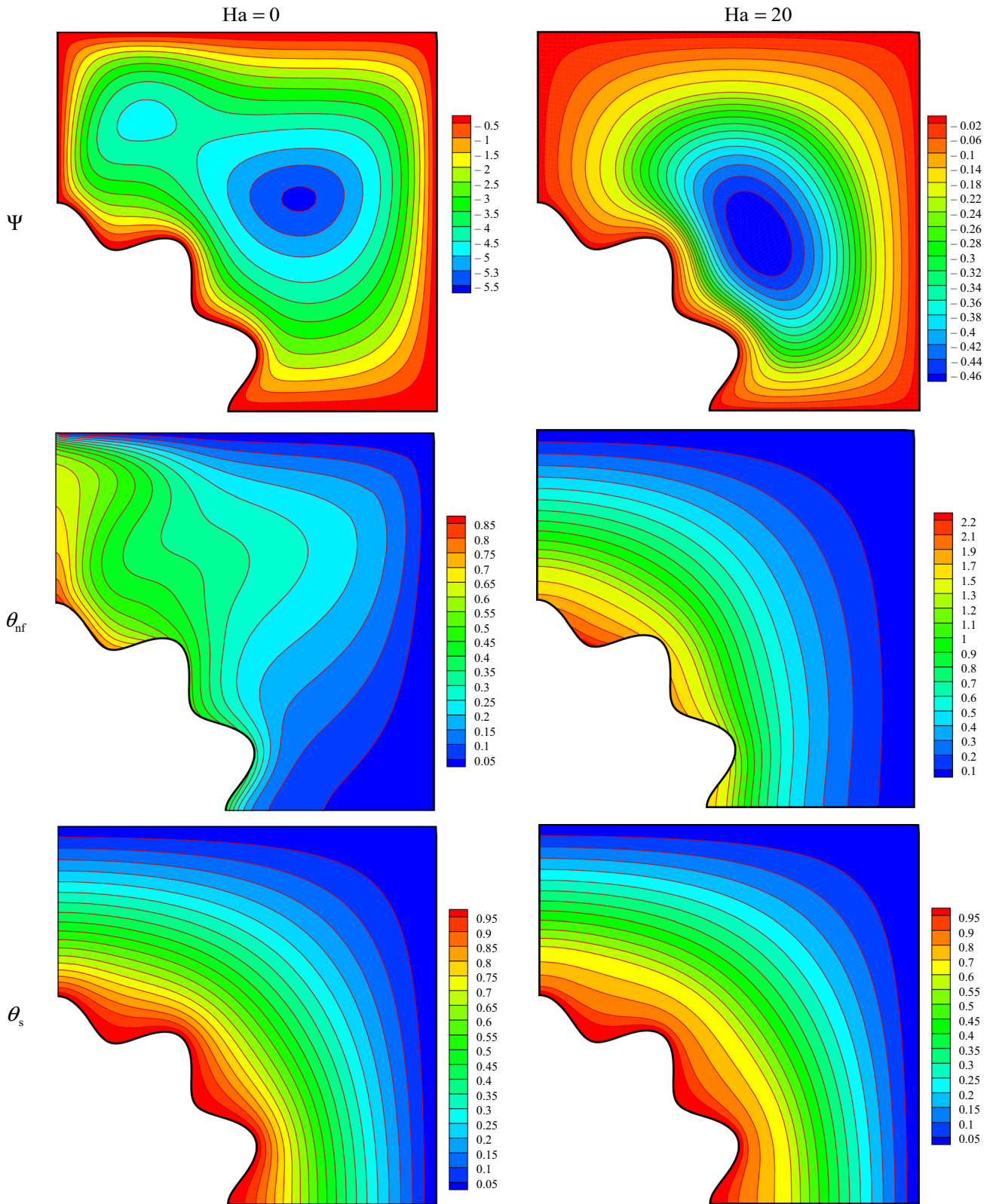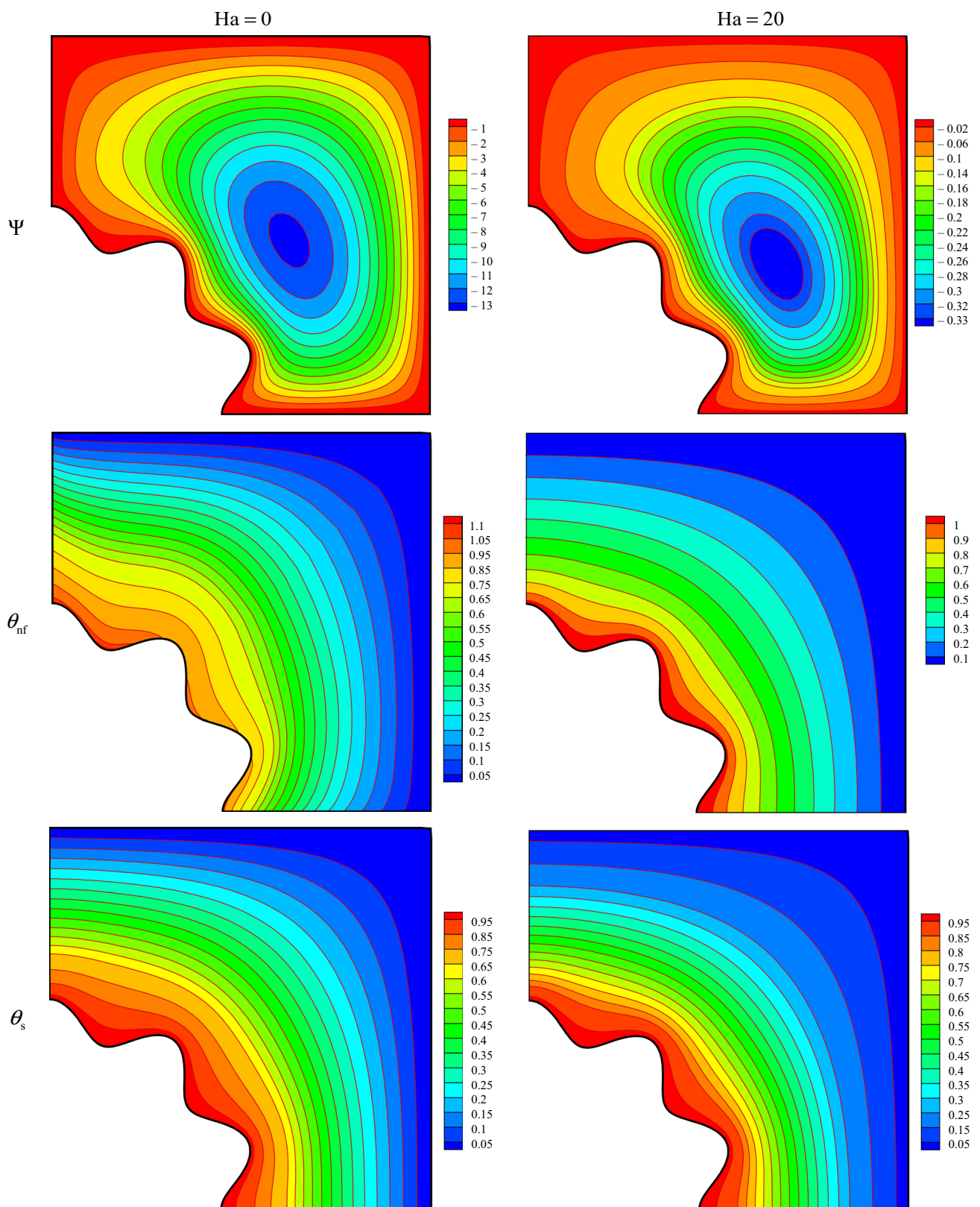
Fig. 5 Contours of (Ψ), (θ_{nf}) and (θ_s) when $\varepsilon = 0.3$, $\phi = 0.04$, $m = 5.7$, $\mathrm{Ra} = 1000$, $\mathrm{Rd} = 0.8$, $\mathrm{Nhs} = 10$

Fig. 6 Contours of (Ψ), (θ_{nf}) and (θ_s) when Nhs = 1000, $\varepsilon = 0.3$, $\phi = 0.04$, Ra = 1000, Rd = 0.8, m = 5.7
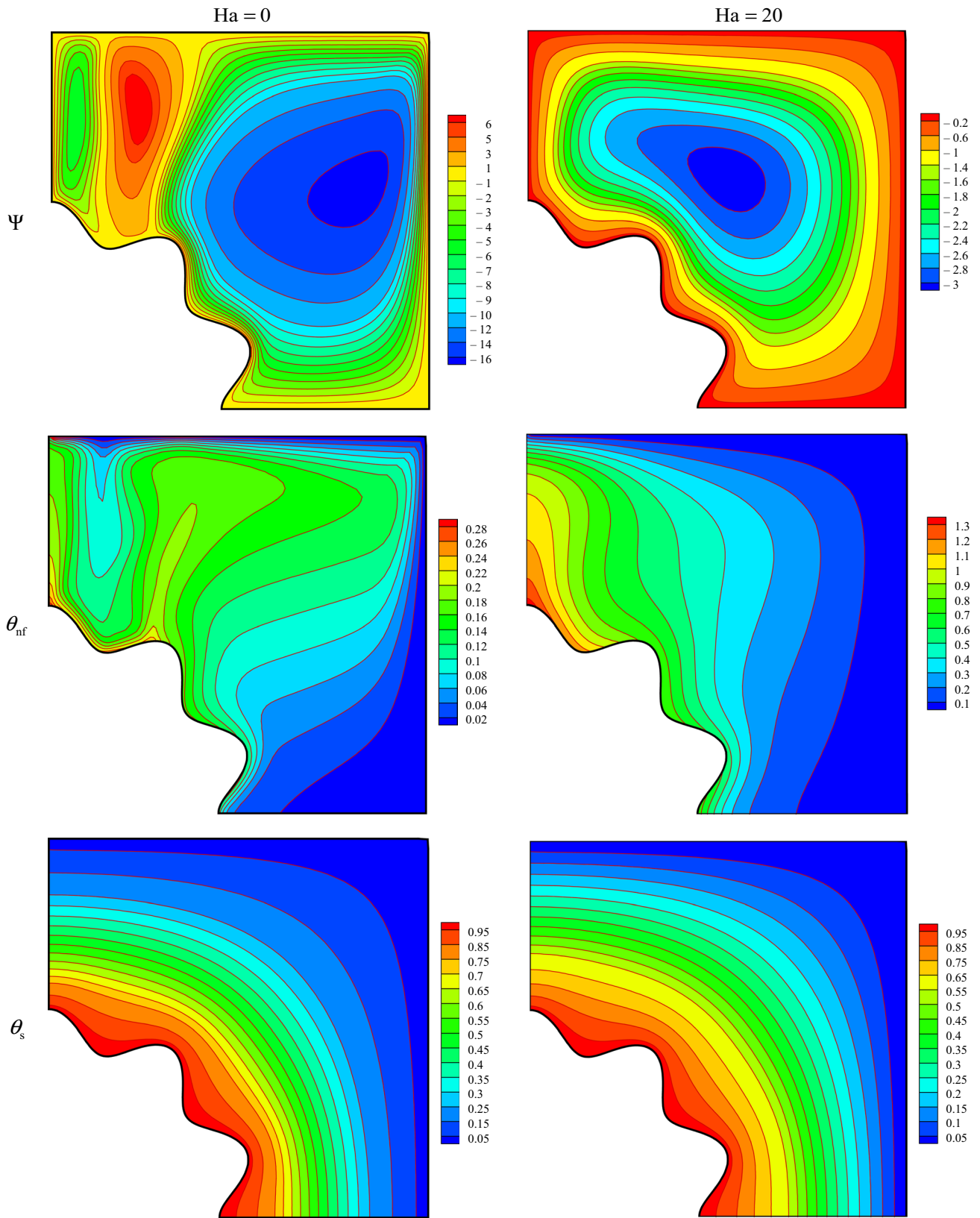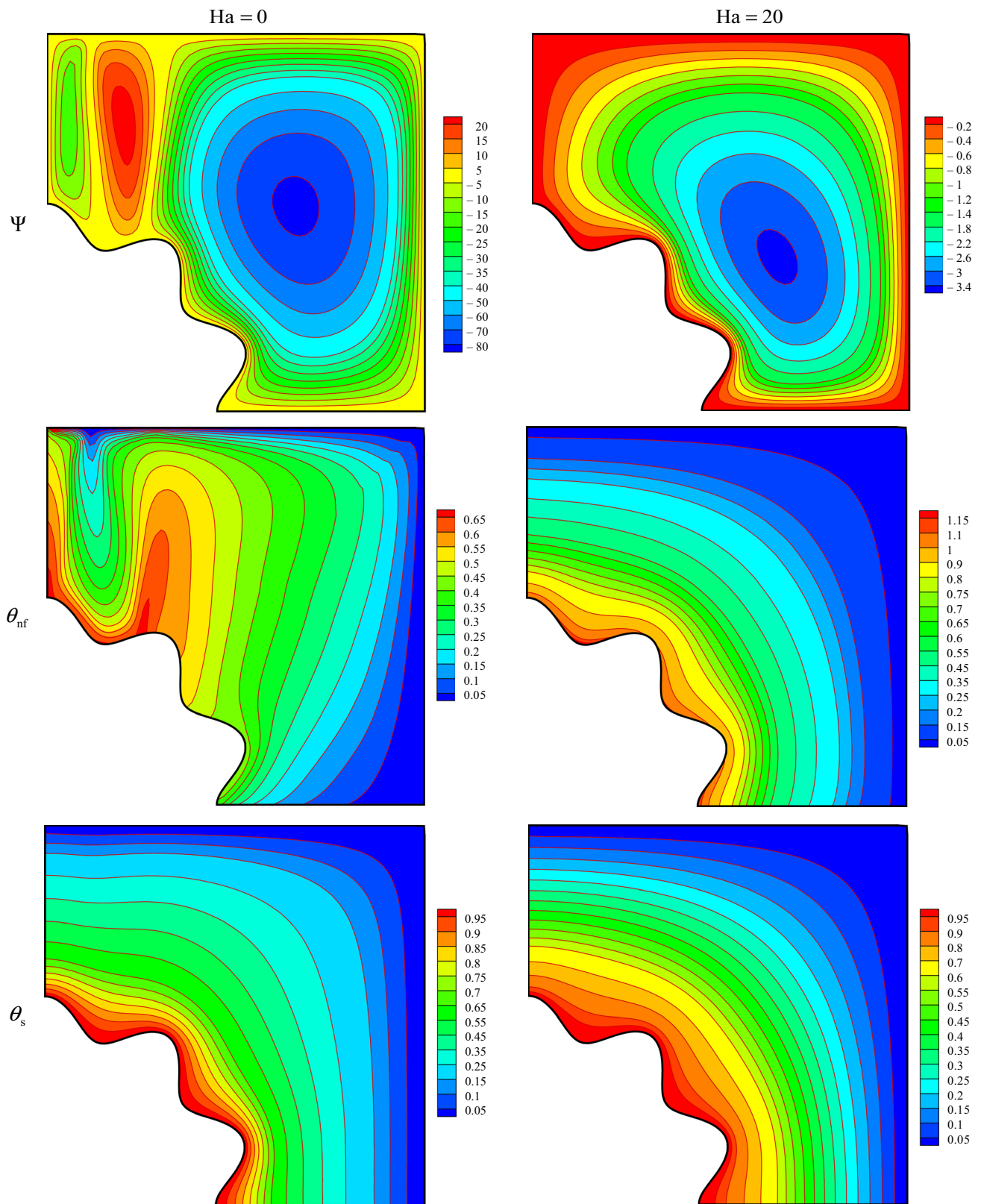
Fig. 7 Contours of (Ψ), (θ_{nf}) and (θ_s) when $\varepsilon = 0.3$, $\phi = 0.04$, $m = 5.7$, $Rd = 0.8$, $Ra = 10^4$, $Nhs = 10$

Ha = 0

Ha = 20

Ψ

θ_{nf}

θ_s

Fig. 8 Contours of (Ψ), (θ_{nf}) and (θ_s) when Ra = 10^4, $\varepsilon = 0.3$, $\phi = 0.04$, Nhs = 1000, $m = 5.7$, Rd = 0.8

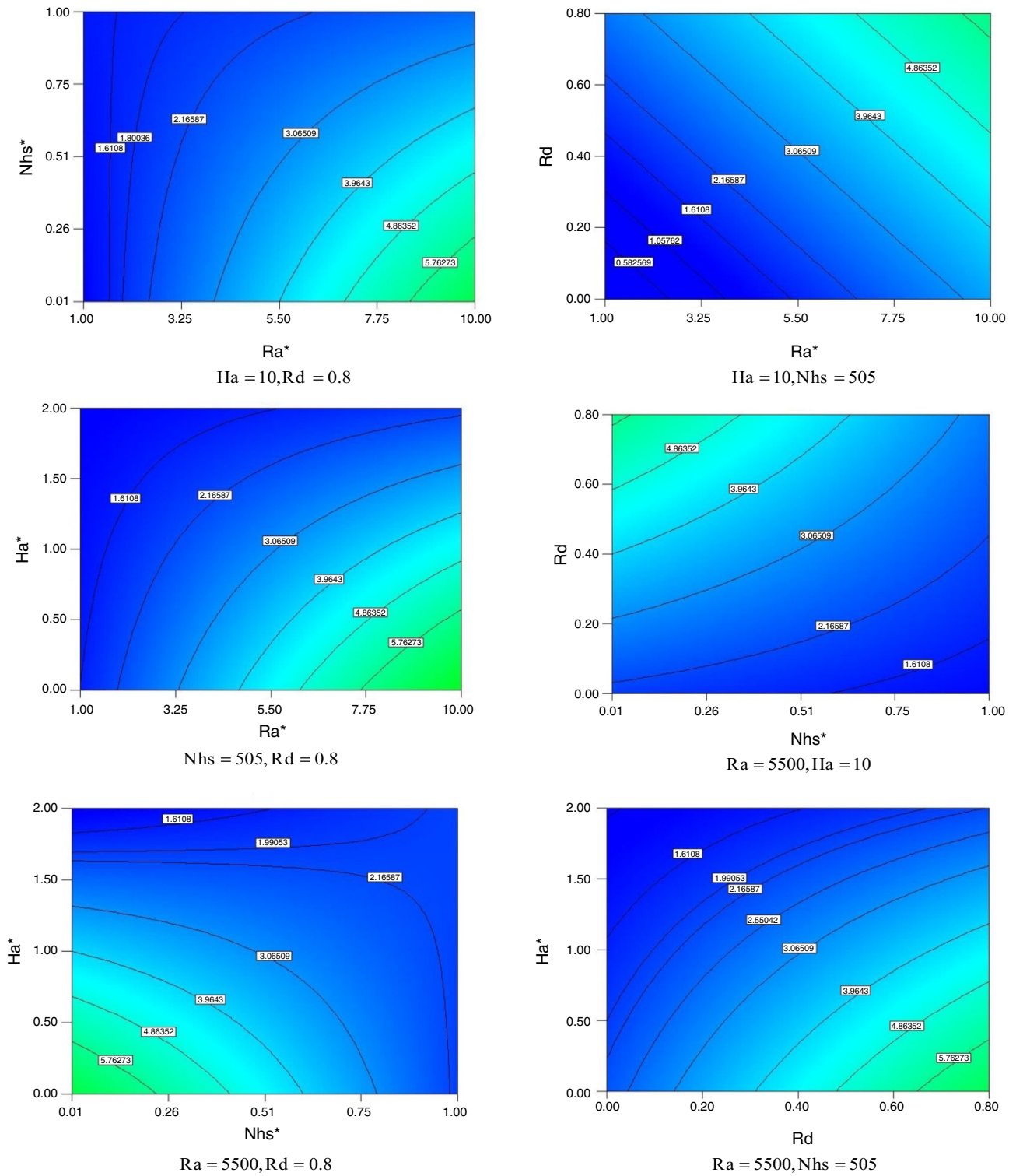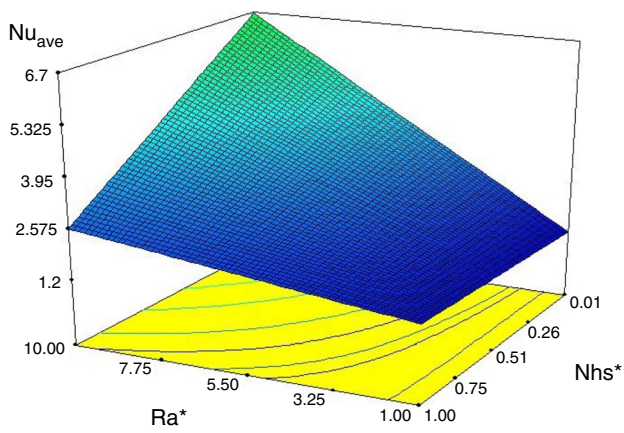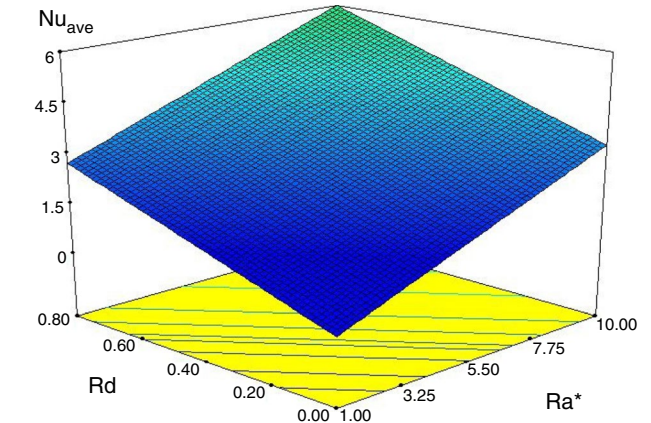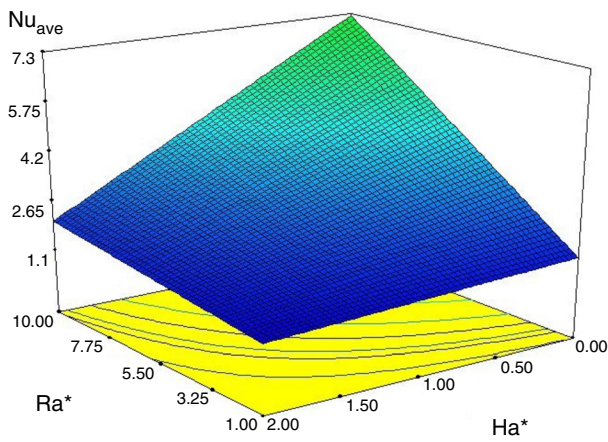**Fig. 9** Influences of Ra, Ha, Rd, Nhs on Nuave at $\varepsilon = 0.3, \phi = 0.04$
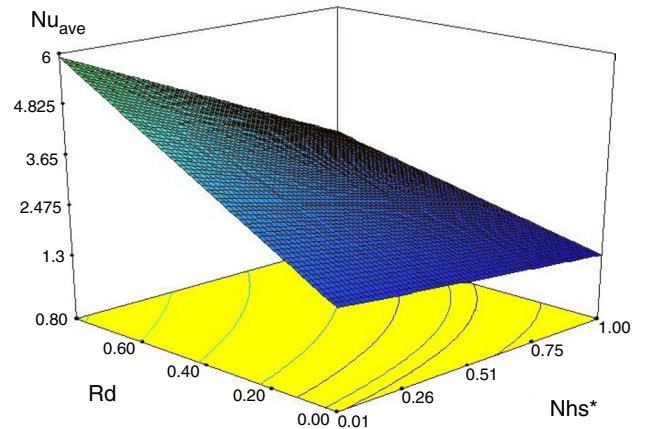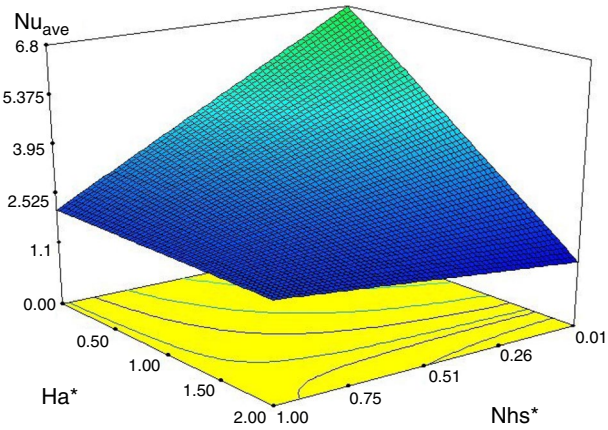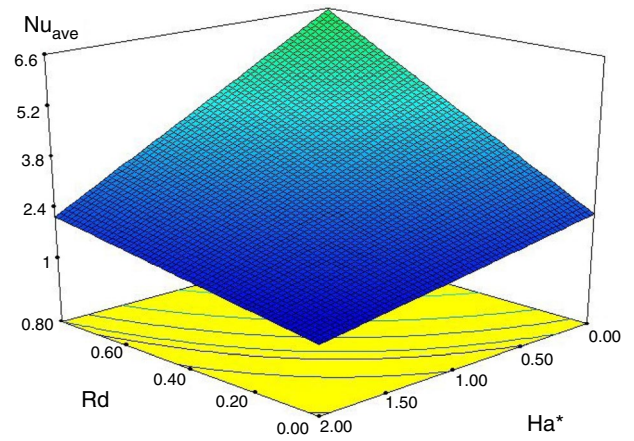
Ha = 10, Rd = 0.8

Ha = 10, Nhs = 505

Nhs = 505, Rd = 0.8

Ra = 5500, Ha = 10

Ra = 5500, Rd = 0.8

Ra = 5500, Nhs = 505

Fig. 9 (continued)

Table 2 Impact of shape of nanoparticles on Nusselt number when Rd = 0.8, Ra = 10, 000, $\varepsilon = 0.3$, Nhs = 10, $\phi = 0.04$

Shape	Ha	
	20	0
Spherical	2.874545	13.5356
Brick	2.911225	13.7089
Cylinder	2.968686	13.98039
Platelet	3.015541	14.2018

its effect reduces with rise of Hartmann number. Spherical shape has minimum heat transfer rate.

Conclusions

In this article, not only the Lorenz force impact but also the radiation impact were analyzed and to simplify the governing equations, Joule heating effect was overlooked and homogeneous model has been employed. As the Nhs is increased, sinusoidal wall temperature augments while increasing Ra has reverse effect. So, Nu$_{ave}$ reduces with augment of Nhs while it rises with rise of Ra. Influence of Ha on temperature profile is converting convection to conduction which provide lower Nu$_{ave}$. According to formula of calculating Nu$_{ave}$, this function has direct relation with Rd. Three eddies are formed inside the domain in absence of magnetic force which intensify the convective flow.

References

1. Rashidi S, Eskandarian M, Mahian O, Poncet S. Combination of nanofluid and inserts for heat transfer enhancement. J Therm Anal Calorim. 2018. https://doi.org/10.1007/s10973-018-7070-9.
2. Mahian O, Kolsi L, Amani M, Estellé P, Ahmadi G, Kleinstreueri C, Marshall JS, Siavash M, Taylor RA, Niazmand H, Wongwises S, Hayat T, Kolanjiyil A, Kasaeian A, Pop I. Recent advances in modeling and simulation of nanofluid flows—part I: fundamentals and theory. Phys Rep. 2019;790(3):1–48.
3. Mahian O, Kolsi L, Amani M, Estellé P, Ahmadi G, Kleinstreueri C, Marshall JS, Siavash M, Taylor RA, Niazmand H, Wongwises S, Hayat T, Kolanjiyil A, Kasaeian A, Pop I. Recent advances in modeling and simulation of nanofluid flows—part II: applications. Phys Rep. 2019;791(13):1–59.
4. Sheikholeslami M. Influence of magnetic field on Al$_2$O$_3$–H$_2$O nanofluid forced convection heat transfer in a porous lid driven cavity with hot sphere obstacle by means of LBM. J Mol Liq. 2018;263:472–88.
5. Qin Y, He Y, Wu B, Ma S, Zhang X. Regulating top albedo and bottom emissivity of concrete roof tiles for reducing building heat gains. Energy Build. 2017;156(3):218–24.
6. Sheikholeslami M. Numerical simulation for solidification in a LHTESS by means of Nano-enhanced PCM. J Taiwan Inst Chem Eng. 2018;86:25–41.
7. Sheikholeslami M. Numerical modeling of nano enhanced PCM solidification in an enclosure with metallic fin. J Mol Liq. 2018;259:424–38.
8. Yang L, Du K. A comprehensive review on the natural, forced and mixed convection of non-Newtonian fluids (nanofluids) inside different cavities. J Therm Anal Calorim. 2019. https://doi.org/10.1007/s10973-019-08987-y.
9. Sheikholeslami M, Shamlooei M. Fe$_3$O$_4$–H$_2$O nanofluid natural convection in presence of thermal radiation. Int J Hydrog Energy. 2017;42(9):5708–18.
10. Sheikholeslami M, Rokni HB. Magnetic nanofluid flow and convective heat transfer in a porous cavity considering Brownian motion effects. Phys Fluids. 2018. https://doi.org/10.1063/1.5012517.
11. Qin Y, Zhang M, Mei G. A new simplified method for measuring the permeability characteristics of highly porous media. J Hydrol. 2018;562:725–32.
12. Sheikholeslami M, Jafaryar M, Hedayat M, Shafee A, Li Z, Nguyen TK, Bakouri M. Heat transfer and turbulent simulation of nanomaterial due to compound turbulator including irreversibility analysis. Int J Heat Mass Transf. 2019;137:1290–300.
13. Ma X, Sheikholeslami M, Jafaryar M, Shafee A, Nguyen-Thoi T, Li Z. Solidification inside a clean energy storage unit utilizing phase change material with copper oxide nanoparticles. J Clean Prod. 2019. https://doi.org/10.1016/j.jclepro.2019.118888.
14. Sheikholeslami M, Mahian O. Enhancement of PCM solidification using inorganic nanoparticles and an external magnetic field with application in energy storage systems. J Clean Prod. 2019;215:963–77.
15. Sheikholeslami M, Ellahi R. Three dimensional mesoscopic simulation of magnetic field effect on natural convection of nanofluid. Int J Heat Mass Transf. 2015;89:799–808.
16. Sheikholeslami M, Jafaryar M, Shafee A, Li Z, Haq R. Heat transfer of nanoparticles employing innovative turbulator considering entropy generation. Int J Heat Mass Transf. 2019;136:1233–40.
17. Guestala M, Kadjaa M, Hoangb MT. Study of heat transfer by natural convection of nanofluids in a partially heated cylindrical enclosure. Case Stud Therm Eng. 2018;11:135–44.
18. Arul Kumar R, Ganesh Babu B, Mohanraj M. Thermodynamic performance of forced convection solar air heaters using pin-fin absorber plate packed with latent heat storage materials. J Therm Anal Calorim. 2016;126:1657–78.
19. Sheikholeslami M, Shehzad SA. Magnetohydrodynamic nanofluid convection in a porous enclosure considering heat flux boundary condition. Int J Heat Mass Transf. 2017;106:1261–9.
20. Sheikholeslami M, Rokni HB. Simulation of nanofluid heat transfer in presence of magnetic field: a review. Int J Heat Mass Transf. 2017;115:1203–33.
21. Vo DD, Hedayat M, Ambreen T, Shehzad SA, Sheikholeslami M, Shafee A, Nguyen TK. Effectiveness of various shapes of Al$_2$O$_3$ nanoparticles on the MHD convective heat transportation in porous medium: CVFEM modeling. J Therm Anal Calorimet. 2019. https://doi.org/10.1007/s10973-019-08501-4.
22. Sheikholeslami M, Li Z, Shafee A. Lorentz forces effect on NEPCM heat transfer during solidification in a porous energy storage system. Int J Heat Mass Transf. 2018;127:665–74.
23. Sheikholeslami M, Jafaryar M, Saleem S, Li Z, Shafee A, Jiang Y. Nanofluid heat transfer augmentation and exergy loss inside a pipe equipped with innovative turbulators. Int J Heat Mass Transf. 2018;126:156–63.
24. Sheikholeslami M, Ghasemi A, Li Z, Shafee A, Saleem A. Influence of CuO nanoparticles on heat transfer behavior of PCM in solidification process considering radiative source term. Int J Heat Mass Transf. 2018;126:1252–64.

25. Meibodi SS, Kianifar A, Mahian O, Wongwises S. Second law analysis of a nanofluid-based solar collector using experimental data. J Therm Anal Calorim. 2016;126:617–25.

26. Sheikholeslami M, Darzi M, Li Z. Experimental investigation for entropy generation and exergy loss of nano-refrigerant condensation process. Int J Heat Mass Transf. 2018;125:1087–95.

27. Sheikholeslami M, Shehzad SA, Li Z. Water based nanofluid free convection heat transfer in a three dimensional porous cavity with hot sphere obstacle in existence of Lorenz forces. Int J Heat Mass Transf. 2018;125:375–86.

28. Bellos E, Tzivanidis C. Thermal efficiency enhancement of nanofluid-based parabolic trough collectors. J Therm Anal Calorim. 2018. https://doi.org/10.1007/s10973-018-7056-7.

29. Stalin PMJ, Arjunan TV, Matheswaran MM, Sadanandam N. Experimental and theoretical investigation on the effects of lower concentration CeO_2/water nanofluid in flat-plate solar collector. J Therm Anal Calorim. 2017. https://doi.org/10.1007/s10973-017-6865-4.

30. Sheikholeslami M, Ghasemi A. Solidification heat transfer of nanofluid in existence of thermal radiation by means of FEM. Int J Heat Mass Transf. 2018;123:418–31.

31. Sheikholeslami M, Rezaeianjouybari B, Darzi M, Shafee A, Li Z, Nguyen TK. Application of nano-refrigerant for boiling heat transfer enhancement employing an experimental study. Int J Heat Mass Transf. 2019;141:974–80.

32. Y. Qin, H. He, A new simplified method for measuring the albedo of limited extent targets, Solar Energy 157(Supplement C) (2017) 1047-1055.

33. Sheikholeslami M. Application of Darcy law for nanofluid flow in a porous cavity under the impact of Lorentz forces. J Mol Liq. 2018;266:495–503.

34. Sheikholeslami M, Arabkoohsar A, Jafaryar M. Impact of a helical-twisting device on nanofluid thermal hydraulic performance of a tube. J Therm Anal Calorim. 2019. https://doi.org/10.1007/s10973-019-08683-x.

35. Sheikholeslami M, Rokni HB. Numerical simulation for impact of Coulomb force on nanofluid heat transfer in a porous enclosure in presence of thermal radiation. Int J Heat Mass Transf. 2018;118:823–31.

36. Selimefendigil F, Ismael MA, Chamkha AJ. Mixed convection in superposed nanofluid and porous layers in square enclosure with inner rotating cylinder. Int J Mech Sci. 2017;124–125:95–108.

37. Korres DN, Tzivanidis C, Koronaki IP, Nitsas MT. Experimental, numerical and analytical investigation of a U-type evacuated tube collectors' array. Renew Energy. 2019;135:218–31.

38. Sheikholeslami M. Finite element method for PCM solidification in existence of CuO nanoparticles. J Mol Liq. 2018;265:347–55.

39. Sheikholeslami M. Solidification of NEPCM under the effect of magnetic field in a porous thermal energy storage enclosure using CuO nanoparticles. J Mol Liq. 2018;263:303–15.

40. Jouybari BR, Osgouie KG, Meghdari A. Optimization of kinematic redundancy and workspace analysis of a dual-arm cam-lock robot. Robotica. 2016;34(1):23–42.

41. Seyednezhad M, Sheikholeslami M, Ali JA, Shafee A, Nguyen TK. Nanoparticles for water desalination in solar heat exchanger: a review. J Therm Anal Calorimet. 2019. https://doi.org/10.1007/s10973-019-08634-6.

42. Sheikholeslami M, Gerdroodbary MB, Shafee A, Tlili I. Hybrid nanoparticles dispersion into water inside a porous wavy tank involving magnetic force. J Therm Anal Calorimet. 2019. https://doi.org/10.1007/s10973-019-08858-6.

43. B. Rezaeianjouybari, K.G. Osgouie, A. Meghdari. Employing neural networks for manipulability optimization of the dual-arm cam-lock robot. In: ASME international mechanical engineering congress and exposition, proceedings (IMECE), 2010, vol. 8.

44. Manh TD, Nam ND, Abdulrahman GK, Moradi R, Babazadeh H. Impact of MHD on hybrid nanomaterial free convective flow within a permeable region. J Therm Anal Calorimet. 2019. https://doi.org/10.1007/s10973-019-09008-8.

45. Qin Y, Hiller JE, Meng D. Linearity between pavement thermophysical properties and surface temperatures. J Mater Civ Eng. 2019. https://doi.org/10.1061/(ASCE)MT.1943-5533.0002890.

46. Sheikholeslami M, Rokni HB. Melting heat transfer influence on nanofluid flow inside a cavity in existence of magnetic field. Int J Heat Mass Transf. 2017;114:517–26.

47. Li Y, Aski FS, Barzinjy AA, Dara RN, Shafee A, Tlili I. Nanomaterial thermal treatment along a permeable cylinder. J Therm Anal Calorimet. 2019. https://doi.org/10.1007/s10973-019-08706-7.

48. Farshad SA, Sheikholeslami M. Simulation of exergy loss of nanomaterial through a solar heat exchanger with insertion of multi-channel twisted tape. J Therm Anal Calorimet. 2019;138:795–804. https://doi.org/10.1007/s10973-019-08156-1.

49. Yang L, Ji W, Huang JN, Xu G. An updated review on the influential parameters on thermal conductivity of nano-fluids. J Mol Liq. 2019;296:111780.

50. Sheikholeslami M, Sadoughi MK. Simulation of CuO–water nanofluid heat transfer enhancement in presence of melting surface. Int J Heat Mass Transf. 2018;116:909–19.

51. Qin Y, Luo J, Chen Z, Mei G, Yan L-E. Measuring the albedo of limited-extent targets without the aid of known-albedo masks. Sol Energy. 2018;171:971–6.

52. Tlili I, Alkanhal TA, Othman M, Dara RN, Shafee A. Water management and desalination in KSA view 2030: case study of solar humidification and dehumidification system. J Therm Anal Calorimet. 2019. https://doi.org/10.1007/s10973-019-08700-z.

53. Sheikholeslami M, Seyednezhad M. Nanofluid heat transfer in a permeable enclosure in presence of variable magnetic field by means of CVFEM. Int J Heat Mass Transf. 2017;114:1169–80.

54. Sheikholeslami M, Jafaryar M, Shafee A, Li Z. Nanofluid heat transfer and entropy generation through a heat exchanger considering a new turbulator and CuO nanoparticles. J Therm Anal Calorim. 2019. https://doi.org/10.1007/s10973-018-7866-7.

55. Sheikholeslami M, Shehzad SA. CVFEM for influence of external magnetic source on Fe_3O_4–H_2O nanofluid behavior in a permeable cavity considering shape effect. Int J Heat Mass Transf. 2017;115:180–91.

56. Yang L, Mao M, Huang JN, Ji W. Enhancing the thermal conductivity of SAE 50 engine oil by adding zinc oxide nano-powder: an experimental study. Powder Technol. 2019;356:335–41.

57. Bianco V, Scarpa F, Tagliafico LA. Numerical analysis of the Al_2O_3–water nanofluid forced laminar convection in an asymmetric heated channel for application in flat plate PV/T collector. Renew Energy. 2018;116:9–21.

58. Rafatijo H, Monge-Palacios M, Thompson DL. Identifying collisions of various molecularities in molecular dynamics simulations. J Phys Chem A. 2019;123(6):1131–9. https://doi.org/10.1021/acs.jpca.8b11686.

59. Rafatijo H, Thompson DL. General application of Tolman's concept of activation energy. J Chem Phys. 2017;147:224111. https://doi.org/10.1063/1.5009751.

60. Qin Y, He Y, Hiller JE, Mei G. A new water-retaining paver block for reducing runoff and cooling pavement. J Clean Prod. 2018;199:948–56.

61. Sheikholeslami M, Sadoughi M. Mesoscopic method for MHD nanofluid flow inside a porous cavity considering various shapes of nanoparticles. Int J Heat Mass Transf. 2017;113:106–14.

62. Sheikholeslami M, Bhatti MM. Forced convection of nanofluid in presence of constant magnetic field considering shape effects of nanoparticles. Int J Heat Mass Transf. 2017;111:1039–49.

63. Qin Y, Zhao Y, Chen X, Wang L, Li F, Bao T. Moist curing increases the solar reflectance of concrete. Constr Build Mater. 2019;215:114–8.

64. Sheikholeslami M, Haq R, Shafee A, Li Z, Elaraki YG, Tlili I. Heat transfer simulation of heat storage unit with nanoparticles and fins through a heat exchanger. Int J Heat Mass Transf. 2019;135:470–8.

65. Manh TD, Nam ND, Abdulrahman GK, Shafee A, Shamlooei M, Babazadeh H, Jilani AK, Tlili I. Effect of radiative source term on the behavior of nanomaterial with considering Lorentz forces. J Therm Anal Calorimet. 2019. https://doi.org/10.1007/s10973-019-09077-9.

66. Sheikholeslami M, Haq R, Shafee A, Li Z. Heat transfer behavior of nanoparticle enhanced PCM solidification through an enclosure with V shaped fins. Int J Heat Mass Transf. 2019;130:1322–42.

67. Qin Y, Zhang M, Hiller JE. Theoretical and experimental studies on the daily accumulative heat gain from cool roofs. Energy. 2017;129:138–47.

68. Sheikholeslami M, Darzi M, Sadoughi MK. Heat transfer improvement and pressure drop during condensation of refrigerant-based nanofluid: an experimental procedure. Int J Heat Mass Transf. 2018;122:643–50.

69. Sheikholeslami M, Jafaryar M, Jafaryar M, Li Z. Nanofluid turbulent convective flow in a circular duct with helical turbulators considering CuO nanoparticles. Int J Heat Mass Transf. 2018;124:980–9.

70. Qin Y. A review on the development of cool pavements to mitigate urban heat island effect. Renew Sustain Energy Rev. 2015;52:445–59.

71. Sheikholeslami M, Bhatti MM. Active method for nanofluid heat transfer enhancement by means of EHD. Int J Heat Mass Transf. 2017;109:115–22.

72. Sheikholeslami M, Shehzad SA. Thermal radiation of ferrofluid in existence of Lorentz forces considering variable viscosity. Int J Heat Mass Transf. 2017;109:82–92.

73. Sheikholeslami M, Sheremet MA, Shafee A, Li Z. CVFEM approach for EHD flow of nanofluid through porous medium within a wavy chamber under the impacts of radiation and moving walls. J Therm Anal Calorimet. 2019. https://doi.org/10.1007/s10973-019-08235-3.

74. Sheikholeslami M, Rokni HB. Nanofluid two phase model analysis in existence of induced magnetic field. Int J Heat Mass Transf. 2017;107:288–99.

75. Qin Y, He H, Ou X, Bao T. Experimental study on darkening water-rich mud tailings for accelerating desiccation. J Clean Prod. 2019. https://doi.org/10.1016/j.jclepro.2019.118235.

76. Hossain MA, Rees DAS. Natural convection flow of a viscous incompressible fluid in a rectangular porous cavity heated from below with cold sidewalls. Heat Mass Transf. 2003;39(8):657–63.

77. Astanina MS, Abu-Nada E, Sheremet A. Combined effects of thermophoresis, brownian motion and nanofluid variable properties on Cuo–water nanofluid natural convection in a partially heated square cavity. J Heat Transf. 2018;140:082401–12.

78. Ahmad SHA, Saidur R, Mahbubul IM, Al-Sulaiman FA. Optical properties of various nanofluids used in solar collector: a review. Renew Sustain Energy Rev. 2017;73:1014–30.

79. Drummond JE, Korpela SA. Natural convection in a shallow cavity. J Fluid Mech. 1987;182:543–64.

80. Sheikholeslami M, Shehzad SA. Simulation of water based nanofluid convective flow inside a porous enclosure via non-equilibrium model. Int J Heat Mass Transf. 2018;120:1200–12.

81. Sheikholeslami M, Shehzad SA, Li Z, Shafee A. Numerical modeling for Alumina nanofluid magnetohydrodynamic convective heat transfer in a permeable medium using Darcy law. Int J Heat Mass Transf. 2018;127:614–22.

82. Sheikholeslami M. Application of control volume based finite element method (CVFEM) for nanofluid flow and heat transfer. Amsterdam: Elsevier; 2019 **ISBN: 9780128141526**.

83. Sheikholeslami M, Shehzad SA. CVFEM simulation for nanofluid migration in a porous medium using Darcy model. Int J Heat Mass Transf. 2018;122:1264–71.

84. Sheikholeslami M, Seyednezhad M. Simulation of nanofluid flow and natural convection in a porous media under the influence of electric field using CVFEM. Int J Heat Mass Transf. 2018;120:772–81.

85. Alrobaian AA, Alsagri AS, Ali JA, Hamad SM, Shafee A, Nguyen TK, Li Z. Investigation of convective nanomaterial flow and exergy drop considering CVFEM within a porous tank. J Therm Anal Calorimet. 2019. https://doi.org/10.1007/s10973-019-08564-3.

86. Sheikholeslami M. Numerical approach for MHD Al_2O_3–water nanofluid transportation inside a permeable medium using innovative computer method. Comput Methods Appl Mech Eng. 2019;344:306–18.

87. Sheikholeslami M, Shehzad SA. Numerical analysis of Fe_3O_4–H_2O nanofluid flow in permeable media under the effect of external magnetic source. Int J Heat Mass Transf. 2018;118:182–92.

88. Sheikholeslami M. New computational approach for exergy and entropy analysis of nanofluid under the impact of Lorentz force through a porous media. Comput Methods Appl Mech Eng. 2019;344:319–33.

89. Sheikholeslami M, Rokni HB. Numerical modeling of nanofluid natural convection in a semi annulus in existence of Lorentz force. Comput Methods Appl Mech Eng. 2017;317:419–30.

90. Khanafer K, Vafai K, Lightstone M. Buoyancy-driven heat transfer enhancement in a two-dimensional enclosure utilizing nanofluids. Int. J. Heat Mass Transf. 2003;46:3639–53.